A Synthetic Resilin Is Largely Unstructured

Kate M. Nairn,* Russell E. Lyons,† Roger J. Mulder,‡ Stephen T. Mudie,*§ David J. Cookson,§ Emmanuelle Lesieur,† Misook Kim,† Deborah Lau,* Fiona H. Scholes,* and Christopher M. Elvin†

*CSIRO Materials Science and Engineering, Clayton, Victoria, Australia; †CSIRO Livestock Industries, Queensland Bioscience Precinct, St. Lucia, Queensland, Australia; ‡CSIRO Molecular and Health Technologies, Clayton, Victoria, Australia; and §Australian Synchrotron, Clayton, Victoria, Australia

ABSTRACT Proresilin is the precursor protein for resilin, an extremely elastic, hydrated, cross-linked insoluble protein found in insects. We investigated the secondary-structure distribution in solution of a synthetic proresilin (AN16), based on 16 units of the consensus proresilin repeat from *Anopheles gambiae*. Raman spectroscopy was used to verify that the secondary-structure distributions in cross-linked AN16 resilin and in AN16 proresilin are similar, and hence that solution techniques (such as NMR and circular dichroism) may be used to gain information about the structure of the cross-linked solid. The synthetic proresilin AN16 is an intrinsically unstructured protein, displaying under native conditions many of the characteristics normally observed in denatured proteins. There are no apparent α-helical or β-sheet features in the NMR spectra, and the majority of backbone protons and carbons exhibit chemical shifts characteristic of random-coil configurations. Relatively few peaks are observed in the nuclear Overhauser effect spectra, indicating that overall the protein is dynamic and unstructured. The radius of gyration of AN16 corresponds to the value expected for a denatured protein of similar chain length. This high degree of disorder is also consistent with observed circular dichroism and Raman spectra. The temperature dependences of the NH proton chemical shifts were also measured. Most values were indicative of protons exposed to water, although smaller dependences were observed for glycine and alanine within the Tyr-Gly-Ala-Pro sequence conserved in all resilins found to date, which is the site of dityrosine cross-link formation. This result implies that these residues are involved in hydrogen bonds, possibly to enable efficient self-association and subsequent cross-linking. The β-spiral model for elastic proteins, where the protein is itself shaped like a spring, is not supported by the results for AN16. Both the random-network elastomer model and the sliding β-turn model are consistent with the data. The results indicate a flat energy landscape for AN16, with very little energy required to switch between conformations. This ease of switching is likely to lead to the extremely low energy loss on deformation of resilin.

INTRODUCTION

The extreme elasticity of resilin was identified in pioneering studies on the flight mechanisms of insects by Weis-Fogh (1–3), and this early work is reviewed elsewhere (4). These physical properties were attributed to its ''highly amorphous'' nature (5). Resilin was subsequently shown to be involved in jumping mechanisms (6,7), in lens cuticles (8), in walking mechanisms (9), in sound production in cicadas (10), and in the expanding exoskeleton of ticks (11).

Recently, Ardell and Andersen (12) identified a putative resilin gene (*CG15920*) within *Drosophila melanogaster*. Elvin et al. then cloned and expressed the first exon of this gene, to produce a soluble protein, which was cross-linked to form an extremely resilient rubbery hydrogel, rec-1 resilin (13). They also showed that the *CG15920* gene was only expressed during pupal stages, and hence the resilin synthesized at the pupal stage must survive with its extreme elasticity for the lifetime of the adult insect.

We subsequently identified by amino-acid sequence homology another resilin gene within *Anopheles gambiae* (African malaria mosquito). A synthetic construct based on the consensus repeat unit coded for by this gene was developed, and the resulting protein (AN16) was expressed and purified (14). The protein AN16 can also be cross-linked, to give a hydrogel with mechanical properties similar to those of rec-1 resilin. A distinct advantage of AN16 over rec-1 resilin is that the expression yields are greater.

Here we evaluate the structure, and in particular the secondary-structure distribution, within AN16. We discuss our results in relation to the possible structure of natural resilins and also elastin.

Elastin is an important mammalian protein that is similar in many ways to resilin, with at least one significant difference. The similarities include a high resilience that only occurs when the protein is hydrated; cross-linking of a soluble precursor to produce a protein rubber; the repetitive nature of the amino-acid sequences within the proteins; and a high content of glycine and proline. The most obvious difference is in the hydrophobicity of the major repeat units. For example, the major repeat unit of the elastic domain in bovine elastin is (VPGVG), which leads to a very hydrophobic protein overall. In contrast, the repeat unit in AN16, (AQTPSSQYGAP), contains many hydrophilic residues. This implies that the interactions between water and protein in these two systems are likely to be different. This is illustrated by the inverse temperature transition of elastin and elastin-like systems, where the protein coacervates as the temperature is increased.

Submitted August 6, 2007, and accepted for publication March 31, 2008.

Address reprint requests to Kate M. Nairn, CSIRO Materials Science and Engineering, Locked Bag 33, Clayton Sth MDC, Victoria 3169, Australia. E-mail: kate.nairn@csiro.au.

Editor: Kathleen B. Hall.

0006-3495/08/10/3358/08 $2.00

doi: 10.1529/biophysj.107.119107

Resilin does not show this behavior. Nonetheless, understanding the structure of resilins may also shed light on the controversial topic of the structure of elastins. Hence the literature on elastin structure, and in particular the various models proposed to account for elasticity, is briefly outlined below.

In a recent review, Mithieux and Weiss commented, ''No consensus has been reached on the overall structure of elastin'' (15). Without a clear structure for elastin, it is inevitable that the mechanism for elasticity would also be controversial. Some studies found evidence for a wide range of conformations, with generally a low α-helix content (16,17), whereas others, and in particular Venkatachalam and Urry (18), proposed a β-spiral, i.e., a regular series of type II β-turns. Still other studies (19) (20) found specific structural distributions, or evidence for a significant fraction of polyproline II helix within the secondary structure (21). The elastin systems evaluated have included tissue (22), tropoelastins (before cross-linking) (20), model polypeptides based on typical repeat units (23), small synthetic peptides in solutions (24), and small, freeze-dried peptides (19).

The β-spiral model was originally developed from the crystal structure of a cyclic model peptide, cyclo$(VPGVG)_3$ (18). The solution NMR spectra of this cyclic peptide resembled the spectra of the linear polypentapeptide based on the VPGVG repeat unit of the hydrophobic domain of bovine elastin, $(VPGVG)_n$ (25). Features consistent with β-spirals were observed in atomic force microscopy studies of the high-molecular-weight subunit of gluten (25,26). The elasticity mechanism associated with this proposed structure is essentially that, in the unstretched state, regions of the chain are relatively free to swing from side-to-side (''librate''), whereas when stretched, these librations are restricted, reducing the entropy of the system (27). Elastic recoil is associated with the restoration of entropy.

Rubber-like elasticity was also proposed for elastic proteins (28,29). This mechanism requires that the polymer chains in the relaxed state can sample a wide range of conformations (i.e., that the polymer system is highly disordered), and that the change in internal energy associated with changing the length of the sample is small. When the rubber is deformed, the range of conformations available to the chains is reduced. Again, as with the β-spiral model, elastic recoil is associated with the restoration of entropy. A number of studies found little evidence for structure in solid elastin (29), in elastin domains in solution (30), and in model polypeptides (23).

Some studies found a particular conformational distribution, rather than a single spiral structure, or complete disorder. For example, Toonkool et al. (20) used sedimentation velocity measurements on human tropoelastin solutions to find a compact and an extended shape of the tropoelastin. Yao and Hong (19) evaluated the small peptide $(VPGVG)_3$ using solid-state NMR, and found two distinct shapes for the central Pro-Gly residues within the repeat: one compact, and the other more extended. Neither of these shapes was consistent with a β-spiral. This peptide displays the same NMR chemical shifts as large polypeptides based on the VPGVG unit (31), and hence provides a reasonable model for the polypeptide structure.

Tamburro et al. (21) embarked on an ''exon-by-exon dissection'' of human tropoelastin. In the course of this process, they evaluated the structure in solution of a broad range of peptides coded for by the human tropoelastin gene (24,32–35). In many of these peptides, they found evidence for polyproline II conformations in equilibrium with a disordered state (21,36,37). In more hydrophobic environments, various β-turns also occur. These conformations have fluctuated, again supporting the idea that polymer chains in elastin sample a broad range of conformations, and rapidly change between extended and compact states. The β-turns were proposed to be labile, and able to slide along the chain (38). These ''sliding β-turns'' increase the entropy of the chain. Deforming the protein is proposed to restrict the sliding and hence reduce the entropy; restoration of this entropy is again associated with elastic recoil.

An alternative mechanism for elasticity in elastin is that of hydrophobic hydration (39–41). This mechanism suggests that deforming the protein brings hydrophobic side chains into contact with water, and that removal of this unfavorable interaction is the driving force for elastic recoil. If this mechanism were dominant, it might be expected that resilin, which has substantially fewer hydrophobic side chains than elastin, would be less elastic than elastin. This is not the case (13), and hence this mechanism is unlikely to apply to both resilin and elastin.

Hence a significant difference between the proposed models for elastin is the presence or absence of regular structural motifs within the protein. In particular, stable β-turns, which can be characterized via NMR through the close approach of the α-carbons at residues i and $i + 3$ of the turn, are required for the β-spiral model. The presence of more labile β-turns may support the sliding β-turn model. A high degree of disorder supports models based on rubber-like elasticity, but does not exclude the sliding β-turn model or those models where an ordered state rapidly exchanges with a disordered one.

We used a range of experimental techniques to evaluate the structure of a synthetic resilin, AN16, both as a cross-linked hydrated gel and as an uncross-linked proresilin in solution. The cross-linked gel and the uncross-linked proresilin at both high (200 mg/mL) and moderate (30 mg/mL) concentrations had similar Raman spectra, and hence similar secondary-structure distributions. Because it is more straightforward to evaluate the protein in solution than as a cross-linked gel, we focused on the secondary structure of the proresilin before cross-linking.

MATERIALS AND METHODS

Protein preparation

An *A. gambiae* homologue (GenBank accession number BX619161) of the *D. melanogaster* resilin gene was identified by protein query versus trans-

lated database (tblastn) analysis of expressed sequence tags databases (42). Alignment of the predicted amino-acid sequence within the repetitive domain of the *A. gambiae* cDNA resulted in an 11-residue consensus sequence, AQTPSSQYGAP. This consensus motif was based on the most common amino acid at each position, relative to the fully conserved YGAP motif.

The construct design was developed by modification of a method for generating periodic polypeptides of a gliadin repeat motif (43). The preparation and characterization of the initial primer modules, their combination by repetitive doubling to produce a 16-copy construct, and the procedures for expression of the corresponding protein in *Escherichia coli* and for subsequent cell disruption were described previously (14). The final designed protein sequence is MHHHHHHP(GAPAQTPSSQY)$_{16}$V, with a molecular mass of 18,578 Da, and 185 residues in total.

After protein expression and cell disruption, the soluble protein fraction was recovered in supernatant, and the recombinant proresilin was purified as previously described (14). Briefly, recombinant protein was partially purified from the clarified soluble fraction by precipitation in 20% ammonium sulfate, and the precipitated pellets were resuspended in sterile phosphate-buffered saline (PBS, pH 7) and dialyzed overnight at 4°C in excess PBS to remove ammonium sulfate. This protein was then heated with stirring for 15 min at 80°C, and denatured proteins were removed by centrifugation. The supernatant was then stored at −80°C. Purity and recovery rates were assessed by sodium dodecyl sulfate polyacrylamide gel electrophoresis analysis. Polyacrylamide gels were fixed and stained with either Coomassie brilliant blue R-250 or silver nitrate (44).

Raman spectra

An inVia confocal microscope system (Renishaw, Gloucestershire, UK) was used, with 830 nm excitation from a diode laser through a 50× long working distance objective (numerical aperture, 0.55), at an incident power of either 150 or 300 mW. Coaxial backscattering geometry was used. Spectra were collected from 500–2500 cm^{-1}, averaged over at least 200 scans. Raman shifts were calibrated using a silicon wafer (peak at 520 cm^{-1}). The spectral resolution was ~1 cm^{-1}.

NMR measurements

A saturated solution of AN16 in a buffer consisting of 37 mM phosphate (Sigma Aldrich, Sydney, Australia) in 9:1 H_2O/D_2O, with 50 mM sodium chloride was used. Spectra were recorded at 5–35°C on a DRX500 spectrometer (Bruker, Rheinstetten, Germany), operating at 500.13 MHz (^{1}H) and 125.6 MHz (^{13}C), with a 5-mm inverse ^{1}H-^{13}C-^{15}N triple-resonance probe. Temperature calibration of the probe was achieved by comparison with ethylene glycol chemical shifts. All ^{1}H and ^{13}C chemical shifts (ppm) were referenced externally to the methyl resonance of sodium 3-(trimethylsilyl)-2,2,3,3-tetradeuteropropionate (TSP, δ 0.00 ppm).

The homonuclear two-dimensional experiments were recorded in phase-sensitive mode, using time-proportional phase increments for quadrature detection (TPPI) in the $t1$ dimension, and included total correlation spectroscopy (TOCSY) using a MLEV-17 spin-lock sequence with a mixing time of 120 ms, and nuclear Overhauser effect (NOE) spectroscopy with a mixing time of 400 ms and double-quantum filtered correlation spectroscopy (DQF-COSY). Solvent suppression for NOESY, TOCSY, and DQF-COSY experiments used presaturation during the relaxation delay of 2 s. Spectra were acquired over 6510 Hz, with 4096 complex data points in the F2 and 512 increments in the F1 dimensions, with 8 scans per increment for TOCSY, 32 for NOE spectroscopy, and 16 scans for DQF-COSY. Spectra were processed using TopSpin version 1.3 software (Bruker, Rheinstetten, Germany). The $t1$ dimension was zero-filled to 2048 real data points, and $\pi/4$ (TOCSY) or $\pi/2$ NOE spectroscopy phase-shifted sine-squared-bell window functions were applied before Fourier transformation. Spectra were analyzed using SPARKY version 3.111 (Goddard and Kneller, University of California, San Francisco, CA). The DQF-COSY $t1$ dimension was zero-filled to 16,384 real data points, and an unshifted sine-bell window function was applied before Fourier transformation. Vicinal H_N-H_α coupling constants were extracted from rows of the DQF-COSY, processed as one-dimensional spectra with a digital resolution of 0.4 Hz/pt.

The heteronuclear single-quantum correlation two-dimensional experiment was recorded in phase-sensitive mode, using echo/antiecho–TPPI for quadrature detection in the $t1$ dimension, with multiplicity editing during the selection step and shaped pulses for improvement of sensitivity (45–47). The ^{13}C chemical shifts were assigned from known ^{1}H chemical shifts.

Small-angle x-ray scattering

Small-angle x-ray scattering (SAXS) data were collected on the SAXS instrument located at sector 15 of ChemMatCARS, at the Advanced Photon Source (Chicago, IL). Details of SAXS measurements and data analysis may be found in the Supplementary Material, Data S1.

RESULTS AND DISCUSSION

Raman spectroscopy

The Raman spectra of the cross-linked gel, the concentrated protein before cross-linking, and a more dilute solution are shown in Fig. 1. An expansion of the amide I region (which is characteristic of the secondary structure) is also presented in Fig. 1. The protein AN16 contains a high concentration of tyrosine residues, which contribute to high background

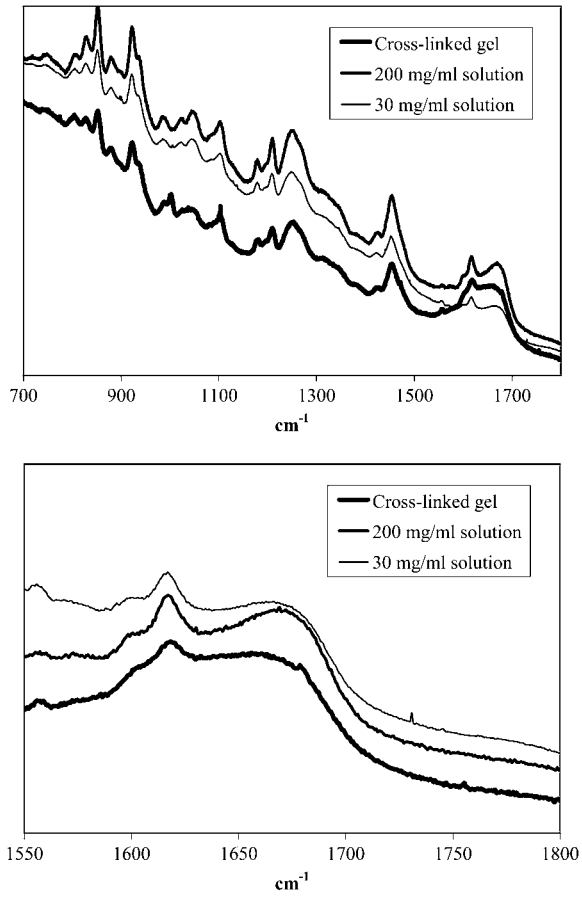

FIGURE 1 (*Top*) Raman spectra for AN16: cross-linked gel, concentrated solution before cross-linking, and more dilute solution. (*Bottom*) Expansion of amide I region.

fluorescence for the protein, resulting in the severely sloping baseline shown in Fig. 1. A band attributable to aromatic side chains (in this case, tyrosine) occurs near the low-frequency edge of the amide I band (around 1615 cm^{-1}), but is not related to the secondary structure of the protein. The broad nature of the amide I bands (centered around 1670 cm^{-1}) indicates a wide range of heterogeneous conformations, and peak deconvolution (not shown) suggests potential contributions from all known secondary structures. All three spectra are similar, implying that the secondary-structure distribution is not greatly affected by protein concentration or by cross-linking. The cross-linked gel has a slightly broader amide I band than the solutions, and hence is likely to adopt an even wider secondary-structure distribution.

NMR spectroscopy

The ^{1}H-^{1}H NOESY and ^{1}H-^{13}C heteronuclear single-quantum correlation spectra of AN16 were assigned from Ala-1 to Pro-11 of the repeat unit (AQTPSSQYGAP). Only one set of resonances was observed (i.e., the data show resonances for Ala-1, rather than 16 different resonances for Ala-1 in each of the repeats of AN16). This could be indicative of either a highly regular structure, with each repeat the same, or a highly mobile structure, where the differences between repeats are averaged out during the course of NMR measurement. Only two tyrosine aromatic proton resonances were observed (a doublet for δ protons at 7.11 ppm, and a doublet for ε protons at 6.81 ppm), which indicates that the rings in Tyr-8 are able to flip freely, implying a significant degree of mobility within the protein.

The chemical shifts for Hα and Cα are plotted as a function of amino-acid sequence in Fig. 2, *a* and *b*. Also shown are the ranges of chemical shifts reported by Zhang et al. (48) for various protein secondary structures. These reference ranges involve the entire range of chemical-shift values observed for a particular residue in a particular secondary-structure environment within their database. Hence if a measured chemical shift is outside the reference range for a particular secondary structure, that residue is unlikely to remain in that conformation for the time required to perform an NMR measurement. The Cα chemical shifts measured for AN16 indicate minimal α-helix content in the protein. The Hα chemical shifts do not support significant β-strand content. This implies that most of the protein is in a random-coil configuration. The exception is Ala-10, which has Cα and Hα chemical shifts indicative of a β-strand or more extended state.

Vicinal H_N-Hα coupling constants are related to the torsion angle subtended between them via a Karplus-like relationship (49). The measured vicinal coupling constants (Fig. 2 *a*) for the AN16 residues (excluding glycine, which was not reported because the two α protons were not resolved) fall in the range of 6.5–8.3 Hz, which excludes stable α-helical or β-sheet structures. These values are consistent with either a randomly fluctuating structure, or a stable polyproline-II-like helix. Vicinal coupling constants for a random coil are taken from Smith et al. (50), and are included for comparison.

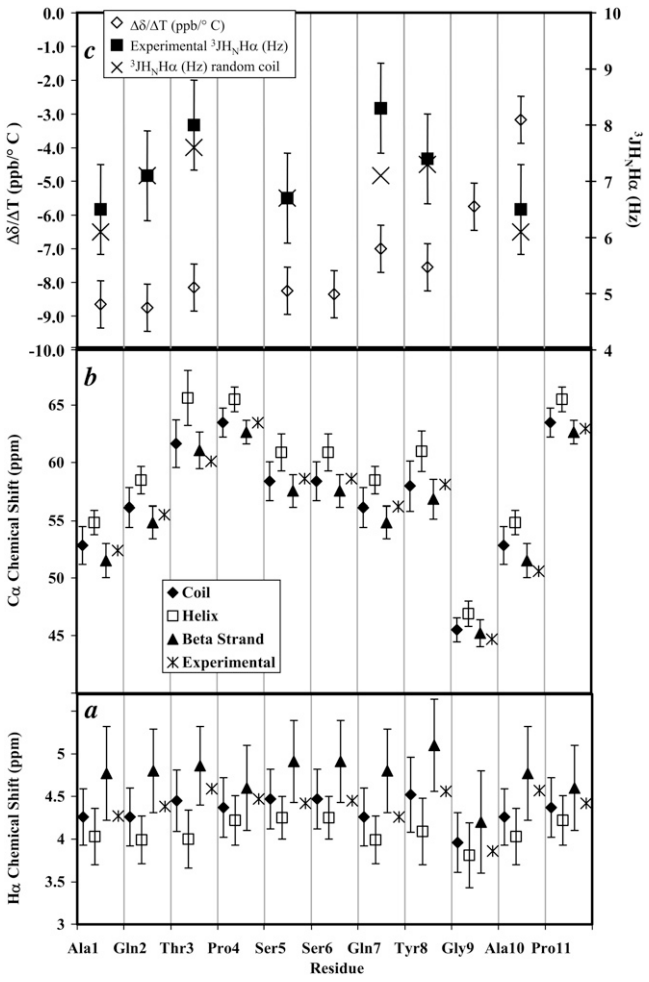

FIGURE 2 The NMR parameters for AN16 at 5°C, plotted versus amino-acid repeat sequence. (*a*) Comparison of experimental Hα chemical shifts, with reference ranges for individual secondary structures from Zhang et al. (48). (*b*) Comparison of experimental Cα chemical shifts, with reference ranges for individual secondary structures from Zhang et al. (48). (*c*) Temperature coefficient of H_N chemical shift (*left axis*), and comparison of experimental $^3JH_NH\alpha$ coupling constants with those predicted by Smith et al. (50) for a random coil (*right axis*).

The NOESY spectrum showed few medium and long-range NOEs. After assigning the intraresidue and sequential peaks, there were 18 other peaks. These are listed in Table 1. The NOE-distances for these peaks were calibrated using the geminal protons of Pro-11 Hδ, Gln-2 Hε, Gln-7 Hε, and Tyr-8 Hβ. Many of these restraints involve Ala-10, suggesting order around that residue. It is difficult to propose a structure that simultaneously brings Ala-10 β-protons close to Ser-5, Ser-6, and Gln-7 β-protons and Tyr-8 δ-protons and ε-protons. Hence all the restraints do not occur within each 11-residue repeat unit. Instead, the Ala-10 environment within the repeat units most likely involves several different conformations.

TABLE 1 ^{1}H-^{1}H NOE restraints for AN16

Residues	Distance ≤2 Å	Distance of 2–4 Å
Ala-1 $Q\beta \leftrightarrow$ Thr-3 H_N		+
Ala-1 $H_N \leftrightarrow$ Thr-3 H_N	+	
Ala-1 $Q\beta \leftrightarrow$ Thr-3 $Q\gamma2$	+	
Thr-3 $H\beta \leftrightarrow$ Ser-6 H_N	+	
Thr-3 $Q\gamma2 \leftrightarrow$ Ala-10 $Q\beta$	+	
Thr-3 $H_N \leftrightarrow$ Gln-7 $H\beta3$	+	
Thr-3 $H\alpha \leftrightarrow$ Gln-7 $H\beta3$	+	
Ser-5 $H_N \leftrightarrow$ Gln-7 $H\beta3$	+	
Ser-5 $H\beta2 \leftrightarrow$ Ala-10 $Q\beta$		+
Ser-6 $H\beta2 \leftrightarrow$ Ala-10 $Q\beta$	+	
Ser-6 $H\alpha \leftrightarrow$ Tyr-8 H_N		+
Ser-6 $H\beta3 \leftrightarrow$ Ala-10 $Q\beta$	+	
Gln-7 $H\beta3 \leftrightarrow$ Ala-10 $Q\beta$		+
Tyr-8 $Q\delta \leftrightarrow$ Ala-10 $Q\beta$		+
Tyr-8 $Q\varepsilon \leftrightarrow$ Ala-10 $Q\beta$		+
Tyr-8 $Q\delta \leftrightarrow$ Pro-11 $H\alpha$	+	
Tyr-8 $Q\varepsilon \leftrightarrow$ Pro-11 $H\alpha$		+
Tyr-8 $H\alpha \leftrightarrow$ Pro-11 $H\delta3$	+	

Q represents a pseudoatom average of multiple hydrogens (in a methyl group or a CH_2, for example). Intraresidue and consecutive correlations were excluded.

Previously, the intensity of sequential NOE peaks was used to identify polyproline II (PPII) structure in peptides based on titin (51). In particular, it was shown that large values of the peak-intensity ratios $\alpha N(i,i+1)/NN(i,i+1)$ and $\alpha N(i,i+1)/\alpha N(i,i)$ are characteristic of PPII. This analysis could not be performed on the current AN16 data, because the peaks in the NOE spectrum overlapped significantly, preventing accurate intensity measurement.

Further evidence for some structure around Ala-10 was obtained from the temperature dependences of the H_N chemical shift, shown in Fig. 2 *c*. Hydrogen bonding typically results in a smaller change in chemical shift with temperature, as was observed for Ala-10, and to a lesser extent Gly-9. The remaining H_N protons exhibit temperature dependences that are characteristic of free, nonhydrogen-bonded residues.

Mackay et al. reported variations in the H_N chemical shift with temperature for ''D26'', a peptide comprising a hydrophobic domain of human tropoelastin (30). For all resolvable H_N peaks, $\Delta\delta H_N/\Delta T$ values of −6 to −8 ppb/K were observed, and interpreted to mean that ''none of the H_N protons are significantly protected from the solvent''. Only two extremely weak nonsequential NOEs were found for D26. In comparison, AN16 exhibits slightly more order, with some protection of certain protons from water (as demonstrated by smaller temperature dependences of the H_N chemical shift), and also more, quite strong, nonsequential NOEs.

SAXS

The radius of gyration for AN16 in solution was found to be 50 (± 5) Å. The exponent of the power-law region of the plot was 2, which is expected for a random coil in solution. Details of the analysis and the original data are in Data S1.

This value of R_g is much greater than expected if AN16 were a globular protein. Narang et al. (52) collated R_g values for globular proteins: a 185-residue globular protein is expected to have an R_g between 14–22 Å. We also do not see the oscillations at higher q values that are typical of folded proteins. Recently, Kohn et al. (53) explored the relationship between R_g and chain length for a wide range of denatured proteins. Their equations give an expected 95% confidence limit R_g range of 33–57 Å for a 185-residue denatured protein, which corresponds to our measured value for AN16.

Overall picture for AN16

The results from our NMR, Raman, and SAXS measurements indicate a high degree of heterogeneity and dynamic disorder within AN16. These data are also consistent with circular dichroism spectra (details in Data S1), which are mostly random-coil, and structure prediction algorithms, such as the predictor of natural disordered regions, PONDr VSL1 (54), that predict the entire protein to be disordered. The NMR data indicate some degree of organization, particularly around Gly-9 and Ala-10. This is within the Tyr-Gly-Ala-Pro sequence conserved in all resilins found to date, which is the site of dityrosine cross-link formation. Molecular motion in this region may be slower to enable efficient self-association and subsequent cross-linking.

Relevance of the structure of AN16 to natural resilin

This study demonstrated the unstructured nature of AN16, a synthetic protein based on the repeat unit of *A. gambiae* resilin, over a range of conditions: dilute and concentrated (200 mg/mL) solutions, and cross-linked gel (200 mg/mL before cross-linking). The synthetic cross-linked gel is known to exhibit the same high resilience as natural resilin (14). Thus it is tempting to translate the unstructured nature of the protein to natural resilin, and suggest that the elasticity of resilin arises from disorder within the protein. However, there are a number of differences between AN16 and natural resilins:

1. AN16 consists almost entirely of perfect repeats. The natural *Anopheles* resilin also contains some nonrepetitive regions, which may affect structure.
2. The concentration of protein in the natural resilin tendons that have been studied to date (such as the dragonfly (1)) is significantly higher than the concentration in our cross-linked gel (40–50% protein, compared to 20%).
3. The solutions in which AN16 was analyzed, and the buffer of the cross-linked gel, are based on human PBS. This does not represent the conditions beneath insect cuticle, where the cells that secrete natural proresilin are located, and where cross-linking occurs. The composition of this region of the insect is currently unknown.
4. Natural resilins are cross-linked via an enzymatic process; the synthetic cross-linked gel was formed by a

photocatalytic process. Although both processes take place via the conversion of tyrosine residues into dityrosine cross-links, the kinetics of the two processes may be very different, and hence the final arrangement of cross-links within the resilins may also differ.

To determine the effects of some of these differences on the structure of resilin, further measurements were performed on samples that more closely approximated the conditions experienced by natural resilin. Either Raman spectroscopy or NMR spectroscopy was used to evaluate the secondary structure in each case. These additional samples included:

1. AN16 gels, formed from solutions that were concentrated (up to 42% protein) before cross-linking. These gels exhibited amide I bands in their Raman spectra (Fig. S4 *a* in Data S1) that were essentially identical to those of the less concentrated gels.
2. AN16 in ''*Drosophila* pupal saline'' solution (6.5 g NaCl, 0.14g KCl, 0.2 g $NaHCO_3$, 0.157 g $CaCl_2{\cdot}2H_2O$, and 0.01 g $NaH_2PO_4{\cdot}2H_2O$ per liter of H_2O/D_2O; personal communication, David Merritt, University of Queensland, St. Lucia, Queensland, Australia). This buffer was chosen because it is likely to approximate the solution conditions under which the proresilin is synthesized. However, as mentioned above, it does not represent the conditions under which cross-linking occurs in vivo. This solution was analyzed by NMR, and no changes in proton chemical shifts of more than 0.02 ppm relative to AN16 in PBS were observed.
3. An uncross-linked sample of AN16, formed by allowing a solution to dry over calcium chloride. This sample exhibited an amide I band in its Raman spectrum (Fig. S4 *b* in Data S1) slightly broader than those observed in the solutions tested.
4. AN16 solutions (150-μL aliquots of around 20% protein in PBS), slowly concentrated further by placing varying amounts (5–80 mg) of polyethylene oxide (MW 600000, Aldrich Chemical Co., Sydney, Australia) in contact with the solutions (by a method similar to the osmotic stress technique described elsewhere (55)). Again, these more concentrated solutions exhibited amide I bands in their Raman spectra (Fig. S4 *b* in Data S1) that were essentially identical to those of the less concentrated solutions.

Hence it was shown that AN16 remains essentially unstructured over a wide range of protein concentrations and also in buffer that represents conditions inside insect cells.

In addition, Raman measurements were performed on a sample of natural resilin, the tendon of a dragonfly, *Aeshna* sp. (gift of Dan Dudek, University of British Columbia, Vancouver, British Columbia, Canada). The actual protein sequence of *Aeshna* resilin is probably very different from that of AN16, because there seems to be a wide variation in resilin sequences from species to species. These tendons were highly fluorescent, and hence difficult to analyze by Raman spectroscopy. The amide I bands obtained (Fig. S4 *c* in Data S1), however, were quite different from the synthetic resilin gels, in that they are narrower, and also appear to have distinct peaks at 1657 and ~1668 cm^{-1}. Although these peaks may arise from additional proteins present within the tendon, the relative narrowness of the amide I band implies that this natural resilin has a narrower distribution of secondary structures than our synthetic resilins. This relative homogeneity may arise from the presence of the other nonrepetitive domains in natural resilin, imposing organization on the repetitive regions. Because both synthetic and natural resilin exhibit high resilience, it is unlikely that changes in the amide I band reflect the structure required for elasticity. Instead, this ordering might contribute to the stiffness of the protein.

Models of elasticity and AN16

The notion that β-turn configurations are critical for elasticity was proposed many years ago. The ''β-spiral'' that was suggested for the high molecular weight subunit of gluten (56) and (somewhat controversially) for elastin (27) is an assembly of repeating β-turns. The data presented here do not support the presence of static β-turns in AN16 because the NOEs that would be expected across the turn were not observed and the NH groups of most residues apparently do not participate in hydrogen bonding. An alternative explanation for the elasticity of elastin involves the ''sliding β-turn'' (38), in which isolated β-turns are able to form and slide along the chain in response to stress. The data presented here do not rule out this mechanism for AN16 resilin.

However, the data are also reasonably consistent with a random-network elastomer model, such as that detailed by Aaron and Gosline for elastin (29), which requires a high degree of disorder within the polymer chains. In particular, the correspondence between the radius of gyration of AN16 and that expected for a denatured protein of similar size is striking.

CONCLUSIONS

We studied AN16 resilin in solution. Some local order was found, particularly around the Tyr-Gly-Ala-Pro motif that is conserved in resilins, and that is the site for the cross-linking reaction.

No evidence was found for a β-spiral structure in resilin. The NMR data suggest that the resilin chains are very mobile, and sample a wide range of conformations. The Raman spectra for AN16 in solution and for AN16 cross-linked gel are similar, which implies that a wide range of conformations is also present within the cross-linked gel, hence supporting elasticity models (such as the sliding β-turn model and the random-network elastomer model) that require disorder.

SUPPLEMENTARY MATERIAL

To view all of the supplemental files associated with this article, visit www.biophysj.org.

We thank the Fairlie Laboratory at the Institute of Molecular Biology, University of Queensland, for the use of their circular dichroism spectrometer. We also thank John Ramshaw, Scott Furman, Vinay Kumar, Jeffrey Church, Anita Hill, and Matthew Hill for helpful discussions, and Connie Darmanin for assistance with SAXS measurements.

This research was supported by a CSIRO Nanotechnology Emerging Sciences Initiative Grant and by the Australian Government through an OzNano2Life Grant. OzNano2life is a project (CG060027) supported by the International Science Linkages Program under the Australian Government's innovation statement Backing Australia's Ability. The SAXS component of this work, including the use of the ChemMatCARS sector, was supported by the Australian Synchrotron Research Program, which is funded by the Commonwealth of Australia under the Major National Research Facilities Program. ChemMatCARS Sector 15 is principally supported by the United States National Science Foundation/Department of Energy under grant CHE0087817. The Advanced Photon Source is supported by the Office of Science, Basic Energy Sciences, United States Department of Energy, under contract W-31-109-Eng-38.

REFERENCES

1. Weis-Fogh, T. 1960. A rubber-like protein in insect cuticle. *J. Exp. Biol.* 37:889–907.
2. Weis-Fogh, T. 1961. Power in flapping flight. *In* The Cell and the Organism. J. Ramsay and V. Wigglesworth, editors. Cambridge UK, University of Cambridge Press. 283–300.
3. Weis-Fogh, T. 1961. Thermodynamic properties of resilin, a rubber-like protein. *J. Mol. Biol.* 3:520–531.
4. Andersen, S. O., and T. Weis-Fogh. 1964. Resilin. A rubberlike protein in arthropod cuticle. *Adv. Insect Physiol.* 2:1–65.
5. Elliott, G. F., A. F. Huxley, and T. Weis-Fogh. 1965. On the structure of resilin. *J. Mol. Biol.* 13:791–795.
6. Gorb, S. N. 2004. The jumping mechanism of cicada *Cercopis vulnerata* (Auchenorrhyncha, Cercopidae): skeleton-muscle organisation, frictional surfaces, and inverse-kinematic model of leg movements. *Arthropod Struct. Dev.* 33:201–220.
7. Bennet-Clark, H. C., and E. C. A. Lucey. 1967. The jump of the flea: a study of the energetics and a model of the mechanism. *J. Exp. Biol.* 47:59–76.
8. Sannasi, A. 1970. Resilin in the lens cuticle of the firefly, *Photinus pyralis* Linnaeus. *Experientia.* 26:154.
9. Neff, D., S. F. Frazier, L. Quimby, R.-T. Wang, and S. Zill. 2000. Identification of resilin in the leg of cockroach, *Periplaneta americana*: confirmation by a simple method using pH dependence of UV fluorescence. *Arthropod Struct. Dev.* 29:75–83.
10. Bennet-Clark, H. C. 1997. Tymbal mechanics and the control of song frequency in the cicada *Cyclochila australasiae*. *J. Exp. Biol.* 200: 1681–1694.
11. Dillinger, S. C. G., and A. B. Kesel. 2002. Changes in the structure of the cuticle of *Ixodes ricinus* L. 1758 (Acari, Ixodidae) during feeding. *Arthropod Struct. Dev.* 31:95–101.
12. Ardell, D. H., and S. O. Andersen. 2001. Tentative identification of a resilin gene in *Drosophila* melanogaster. *Insect Biochem.* 31:965–970.
13. Elvin, C. M., A. G. Carr, M. G. Huson, J. M. Maxwell, R. D. Pearson, T. Vuocolo, N. E. Liyou, D. C. C. Wong, D. J. Merritt, and N. E. Dixon. 2005. Synthesis and properties of crosslinked recombinant proresilin. *Nature.* 437:999–1002.
14. Lyons, R. E., E. Lesieur, M. Kim, D. C. C. Wong, M. G. Huson, K. M. Nairn, A. G. Brownlee, R. D. Pearson, and C. M. Elvin. 2007. Design and facile production of recombinant resilin-like polypeptides: gene construction and a rapid protein purification method. *Protein Eng. Des. Sel.* 20:25–32.
15. Mithieux, S. M., and A. S. Weiss. 2005. Elastin. *Adv. Protein Chem.* 70:437–461.
16. Vrhovski, B., S. Jensen, and A. S. Weiss. 1997. Coacervation characteristics of recombinant human tropoelastin. *Eur. J. Biochem.* 250: 92–98.
17. Debelle, L., A. Alix, S. Wei, M. Jacob, J. Huvenne, M. Berjot, and P. Legrand. 1998. The secondary structure and architecture of human elastin. *Eur. J. Biochem.* 258:533–539.
18. Venkatachalam, C. M., and D. W. Urry. 1981. Development of a linear helical conformation from its cyclic correlate—spiral model of the elastin poly(pentapeptide) $(VPGVG)_n$. *Macromolecules.* 14:1225–1229.
19. Yao, X. L., and M. Hong. 2004. Structure distribution in an elastin-mimetic peptide $(VPGVG)_3$ investigated by solid-state NMR. *J. Am. Chem. Soc.* 126:4199–4210.
20. Toonkool, P., D. G. Regan, P. W. Kuchel, M. B. Morris, and A. S. Weiss. 2001. Thermodynamic and hydrodynamic properties of human tropoelastin. Analytical ultracentrifuge and pulsed field-gradient spin-echo NMR studies. *J. Biol. Chem.* 276:28042–28050.
21. Bochicchio, B., A. Ait-Ali, A. M. Tamburro, and A. J. P. Alix. 2004. Spectroscopic evidence revealing polyproline II structure in hydrophobic, putatively elastomeric sequences encoded by specific exons of human tropoelastin. *Biopolymers.* 73:484–493.
22. Gosline, J. M. 1978. The temperature-dependent swelling of elastin. *Biopolymers.* 17:697–707.
23. Rodriguez-Cabello, J. C., M. Alonso, M. I. Diez, M. I. Caballero, and M. M. Herguedas. 1999. Structural investigation of the poly(pentapeptide) of elastin, poly(GVGVP), in the solid state. *Macromol. Chem. Phys.* 200:1831–1838.
24. Tamburro, A. M., B. Bochicchio, and A. Pepe. 2003. Dissection of human tropoelastin: exon-by-exon chemical synthesis and related conformational studies. *Biochemistry.* 42:13347–13362.
25. Urry, D. W., T. L. Trapane, H. Sugano, and K. U. Prasad. 1981. Sequential polypeptides of elastin: cyclic conformational correlates of the linear polypentapeptide. *J. Am. Chem. Soc.* 103:2080–2089.
26. Miles, M. J., H. J. Carr, T. C. McMaster, K. J. I'Anson, P. S. Belton, V. J. Morris, J. M. Field, P. R. Shewry, and A. S. Tatham. 1991. Scanning tunneling microscopy of a wheat seed storage protein reveals details of an unusual supersecondary structure. *Proc. Natl. Acad. Sci. USA.* 88:68–71.
27. Urry, D. W., and T. M. Parker. 2002. Mechanics of elastin: molecular mechanism of biological elasticity and its relationship to contraction. *J. Muscle Res. Cell Motil.* 23:543–559.
28. Hoeve, C. A., and P. J. Flory. 1974. The elastic properties of elastin. *Biopolymers.* 13:677–686.
29. Aaron, B. B., and J. M. Gosline. 1981. Elastin as a random-network elastomer: a mechanical and optical analysis of single elastin fibers. *Biopolymers.* 20:1247–1260.
30. Mackay, J. P., L. D. Muiznieks, P. Toonkool, and A. S. Weiss. 2005. The hydrophobic domain 26 of human tropoelastin is unstructured in solution. *J. Struct. Biol.* 150:154–162.
31. Hong, M., D. Isailovic, R. A. McMillan, and V. P. Conticello. 2003. Structure of an elastin-mimetic polypeptide by solid-state NMR chemical shift analysis. *Biopolymers.* 70:158–168.
32. Bochicchio, B., N. Floquet, A. Pepe, A. J. P. Alix, and A. M. Tamburro. 2004. Dissection of human tropoelastin: solution structure, dynamics and self-assembly of the exon 5 peptide. *Chem. Eur. J.* 10: 3166–3176.
33. Ostuni, A., M. D. Lograno, A. R. Gasbarro, F. Bisaccia, and A. M. Tamburro. 2002. Novel properties of peptides derived from the sequence coded by exon 26a of human elastin. *Int. J. Biochem. Cell Biol.* 34:130–135.
34. Bisaccia, F., M. A. Castiglione-Morelli, S. Spisani, A. Serafini-Fracassini, and A. M. Tamburro. 2000. Solution structure of the amino acid sequence coded by the rarely expressed exon 26a of human elastin: the N-terminal region. *J. Pept. Res.* 56:201–209.
35. Tamburro, A. M., A. Pepe, B. Bochicchio, D. Quaglino, and I. P. Ronchetti. 2005. Supramolecular amyloid-like assembly of the poly-

peptide sequence coded by exon 30 of human tropoelastin. *J. Biol. Chem.* 280:2682–2690.

36. Martino, M., A. Bavoso, V. Guantieri, A. Coviello, and A. M. Tamburro. 2000. On the occurrence of polyproline II structure in elastin. *J. Mol. Struct.* 519:173–189.
37. Bochicchio, B., and A. M. Tamburro. 2002. Polyproline II structure in proteins: identification by chiroptical spectroscopies, stability, and functions. *Chirality.* 14:782–792.
38. Tamburro, A. M., V. Guantieri, L. Pandolfo, and A. Scopa. 1990. Synthetic fragments and analogues of elastin. II. Conformational studies. *Biopolymers.* 29:855–870.
39. Li, B., D. O. V. Alonso, B. J. Bennion, and V. Daggett. 2001. Hydrophobic hydration is an important source of elasticity in elastin-based biopolymers. *J. Am. Chem. Soc.* 123:11991–11998.
40. Rodriguez-Cabello, J. C., M. Alonso, T. Perez, and M. M. Herguedas. 2000. Differential scanning calorimetry study of the hydrophobic hydration of the elastin-based polypentapeptide, poly(VPGVG), from deficiency to excess of water. *Biopolymers.* 54:282–288.
41. Gosline, J. M. 1976. The physical properties of elastic tissue. *Int. Rev. Connect. Tissue Res.* 7:211–249.
42. Altschul, S. F., T. L. Madden, A. A. Schaffer, J. Zhang, Z. Zhang, W. Miller, and D. J. Lipman. 1997. Gapped BLAST and PSI-BLAST: a new generation of protein database search programs. *Nucleic Acids Res.* 25:3389–3402.
43. Elmorjani, K., M. Thievin, T. Michon, Y. Popineau, J.-N. Hallet, and J. Gueguen. 1997. Synthetic genes specifying periodic polymers modelled on the repetitive domain of wheat gliadins: conception and expression. *Biochem. Biophys. Res. Commun.* 239:240–246.
44. Swain, M., and N. W. Ross. 1995. A silver stain protocol for proteins yielding high resolution and transparent background in sodium dodecyl sulfate-polyacrylamide gels. *Electrophoresis.* 16:948–951.
45. Willker, W., D. Leibfritz, R. Kerssebaum, and W. Bermel. 1993. Gradient selection in inverse heteronuclear correlation spectroscopy. *Magn. Reson. Chem.* 31:287–292.
46. Palmer, A. G. I., J. Cavanagh, P. E. Wright, and M. Rance. 1991. Sensitivity improvement in proton-detected two-dimensional heteronuclear correlation NMR spectroscopy. *J. Magn. Reson.* 93:151–170.
47. Kay, L. E., P. Keifer, and T. Saarinen. 1992. Pure absorption gradient enhanced heteronuclear single quantum correlation spectroscopy with improved sensitivity. *J. Am. Chem. Soc.* 114:10663–10665.
48. Zhang, H., S. Neal, and D. S. Wishart. 2003. RefDB: a database of uniformly referenced protein chemical shifts. *J. Biomol. NMR.* 25:173–195.
49. Wuthrich, K. 1986. NMR of Proteins and Nucleic Acids. Wiley Interscience, New York.
50. Smith, L. J., K. A. Bolin, H. Schwalbe, M. W. Macarthur, J. M. Thornton, and C. M. Dobson. 1996. Analysis of main chain torsion angles in proteins: prediction of NMR coupling constants for native and random coil conformations. *J. Mol. Biol.* 255:494–506.
51. Ma, K., L. S. Kan, and K. Wang. 2001. Polyproline II helix is a key structural motif of the elastic PEVK segment of titin. *Biochemistry.* 40:3427–3438.
52. Narang, P., K. Bhushan, S. Bose, and B. Jayaram. 2005. A computational pathway for bracketing native-like structures for small alpha helical globular proteins. *Phys. Chem. Chem. Phys.* 7:2364–2375.
53. Kohn, J. E., I. S. Millett, J. Jacob, B. Zagrovic, T. M. Dillon, N. Cingel, R. S. Dothager, S. Seifert, P. Thiyagarajan, T. R. Sosnick, M. Z. Hasan, V. S. Pande, I. Ruczinski, S. Doniach, and K. W. Plaxco. 2004. Random-coil behavior and the dimensions of chemically unfolded proteins. *Proc. Natl. Acad. Sci. USA.* 101:12491–12496.
54. Obradovic, Z., K. Peng, S. Vucetic, P. Radivojac, and A. K. Dunker. 2005. Exploiting heterogeneous sequence properties improves prediction of protein disorder. *Proteins.* 61:176–182.
55. Sohn, S., H. H. Strey, and S. P. Gido. 2004. Phase behavior and hydration of silk fibroin. *Biomacromolecules.* 5:751–757.
56. McIntire, T. M., E. J. L. Lew, A. E. Adalsteins, A. Blechl, O. D. Anderson, D. A. Brant, and D. D. Kasarda. 2005. Atomic force microscopy of a hybrid high-molecular-weight glutenin subunit from a transgenic hexaploid wheat. *Biopolymers.* 78:53–61.